Amino Acids (2008) 34:605–616
DOI 10.1007/s00726-007-0014-5

ORIGINAL ARTICLE

Near infrared spectroscopy compared to liquid chromatography coupled to mass spectrometry and capillary electrophoresis as a detection tool for peptide reaction monitoring

Christine H. Petter · Nico Heigl · Stefan Bachmann · Verena A. C. Huck-Pezzei · Muhammad Najam-ul-Haq · Rania Bakry · Andreas Bernkop-Schnürch · Günther K. Bonn · Christian W. Huck

Received: 20 September 2007 / Accepted: 27 November 2007 / Published online: 20 December 2007

Abstract Peptide interaction is normally monitored by liquid chromatography (LC), liquid chromatography coupled to mass spectrometry (LC-MS), mass spectrometric (MS) methods such as MALDI-TOF/MS or capillary electrophoresis (CE). These analytical techniques need to apply either high pressure or high voltages, which can cause cleavage of newly formed bondages. Therefore, near infrared reflectance spectroscopy (NIRS) is presented as a rapid alternative to monitor the interaction of glutathione and oxytocin, simulating physiological conditions. Thereby, glutathione can act as a nucleophile with oxytocin forming four new conjugates via a disulphide bondage. Liquid chromatography coupled to UV (LC-UV) and mass spectrometry via an electrospray ionisation interface (LC-ESI-MS) resulted in a 82% and a 78% degradation of oxytocin at pH 3 and a 5% and a 7% degradation at pH 6.5. Capillary electrophoresis employing UV-detection (CE-UV) showed a 44% degradation of oxytocin. LC and CE in addition to the NIRS are found to be authentic tools for quantitative analysis. Nevertheless, NIRS proved to be highly suitable for the detection of newly formed conjugates after separating them on a thin layer chromatography (TLC) plate. The recorded fingerprint in the near infrared region allows for a selective distinct qualitative identification of conjugates without the need for expensive instrumentation such as quadrupole or MALDI-TOF mass spectrometers. The performance of the established NIRS method is compared to LC and CE; its advantages are discussed in detail.

Keywords Near infrared spectroscopy · Peptides · Reaction monitoring · Liquid chromatography · Mass spectrometry · Capillary electrophoresis

C. H. Petter · N. Heigl · C. W. Huck (✉)
Spectroscopy Group Institute of Analytical Chemistry and Radiochemistry, Leopold-Franzens University, Innrain 52a, 6020 Innsbruck, Austria
e-mail: christian.w.huck@uibk.ac.at

S. Bachmann · V. A. C. Huck-Pezzei · M. Najam-ul-Haq · R. Bakry · G. K. Bonn
Institute of Analytical Chemistry and Radiochemistry, Leopold-Franzens University, Innrain 52a, 6020 Innsbruck, Austria

A. Bernkop-Schnürch
Institute of Pharmacy, Department of Pharmaceutical Technology, Leopold-Franzens University, Innrain 52, 6020 Innsbruck, Austria

Introduction

The discovery of near infrared energy is imputed to William Herschel in the early nineteenth century (Herschel 1800). Initially, near infrared spectroscopy (NIRS) was used as an additional method to study various wavelength regions, aside mid-IR techniques, for example. Today, NIRS is a basic and vastly acclaimed tool for qualitative and quantitative analysis (Chen 2006; Delpy and Cope 1997; Shaw 1996). It is based on molecular overtone and combination transitions of C–H, O–H and N–H groups in a wavenumber ranging from 4,000 to 12,800 cm^{-1} (780–2,500 nm). In the near infrared spectral region, the overtone and combination bands are typically broad, directing to complex spectra. It is, therefore, hard to assign the specific features to specific chemical components (Ciurczak and Drennen 2002). Hence, it is essential to apply the multivariate calibration techniques (e.g., principal component analysis, PCA; partial least squares, PLS; multiple linear regression, MLR; principal component regression,

PCR) for simultaneous analysis of structurally related compounds (Burns and Ciurczak 1992; Esbensen 2001; Forina 1998; Miyazawa and Sonoyama 1998). NIR measurements are based on specific functional group vibrations that constitute an NIR absorption spectrum. The respective signals are just as intense to yield to a particular absorption profile. The NIRS method of analytical investigations is rapid, non-invasive and non-destructive (Barabás 1998; Bokobza 1998). No sample preparation and pre-treatment is required before carrying out the main analysis. There are several studies of applicability and efficiency of NIR spectroscopic detections in pharmaceutical industry, e.g. analysis of intact dosage forms, including chemical, physical and related biopharmaceutical aspects (Sowa 2006; Reich 2003; Huck 1999; Axon 1998). Furthermore, the application of NIRS to measure blood glucose (Amerov 2005), skin lesions (Lauridsen 2003; McIntosh 2001), amino acids (Heigl 2006; Alexander and Tran 2001; De la Haba 2006), peptides (Tran and Kong 2000), proteins (Pezzanitit 2001) and manifold agricultural applications are demonstrated (Fernández-Ahumada 2006; Guggenbichler 2006; Sissons 2006; Huck 2005). Detailed investigations in the proteomics field were carried out by Tran and Kong (2000). They identified amino acid residues in small peptides after sequencing. Shaw et al. (2000) used NIRS for imaging and determination of metalloproteins. Imaging techniques are based upon optical electronic transitions involving the metal centers of hemoglobin (blood), myoglobin (muscle) and cytochrome (mitochondria).

Oxytocin, a nonapeptide which is related to a group of neuropeptides, is secreted in the hypophysis and is vital for contractions during labor, maternal behaviour and social bonding (Huck 2006). For medical purposes, such as to facilitate birth, oxytocin is injected intravenously, intramuscularly or just inhaled. However, the general observation is that the oxytocin has a poor adsorption capacity. Oxytocin reacting with reduced glutathione (GSH, γ-α-glutamyl-α-cysteinylglycine) prevents any absorption into the gastrointestinal tract (GIT); as a result oral administration is impossible. GSH is a tripeptide with a free thiol group and can react as a nucleophile with endogenous and exogenous electrophilic properties. It also plays an important role as antioxidant (Morgenstern and Kirch 2003; Camera and Picardo 2002). The free thiol groups of GSH and oxytocin form a disulfide bridge; thus the emerged complexes cannot cross the sulfhydril barrier in the gastrointestinal tract (Schmitz 2006). Methods most commonly applied to monitor the interaction of glutathione with low molecular weight peptides such as oxytocin comprise reversed-phase liquid chromatography (RPLC) aside capillary electrophoresis. Both methods are time consuming and require a lot of experience. Additionally, RPLC and CE pose the drawback that newly formed conjugates of glutathione and oxytocin might be destabilized by the high pressure or voltage applied before reaching the detector.

Therefore, the aim of the present work is to establish a simple NIRS method for peptide reaction monitoring of oxytocin and glutathione. A qualitative model should allow for rapid identification of newly produced conjugates; a quantitative method is aimed at determining the amount of oxytocin and glutathione degradation without the influence of external parameters such as high pressure and/or voltage. We compare the respective performances of the newly developed NIRS method versus conventional liquid chromatography (LC) coupled to mass spectrometry (MS) as well as capillary electrophoresis (CE) and evaluate the results obtained. Finally, we show that NIRS offers an attractive, non-invasive alternative for peptide reaction monitoring.

Experimental section

Materials and methods

Sodium dihydrogen phosphate (NaH_2PO_4, ≥99.0%), sodium hydroxide (NaOH, ≥98%), acetonitrile (ACN, ≥99.9%), methanol (≥99.9%), pyridine (≥99.0%), phosphoric acid (99%), ammonia, *n*-butanol, pyridine (analytical reagent-grade) and trifluoroacetic acid (TFA, ≥98%) were purchased from Merck (Darmstadt, Germany). Oxytocin, glutathione in reduced (GSH, ≥98%) form, 1,5-dimethyl-l,5diaza-undecamethylene polymethobromide (hexadimethrine bromide, HDB) and Ninhydrin spray reagent were purchased from Sigma Aldrich (Vienna, Austria). Water used was purified by a NANOpure Infinity unit (Barnstead, Boston, MA, USA). Thermostated water bath (variation limit of ±0.1°C) was regulated by a heater (Julabo-model PC/4, Seelbach, Germany).

Preparation of standard solutions

Studies were carried out with 0.05% solutions of oxytocin staggered with solutions of 0.01, 0.1 and 1% GSH at pH 3.0 and 6.5. Buffer solutions at pH 3.0 and 6.5 were created from 1.2 g sodium dihydrogen phosphate or 0.98 g phosphoric acid, dissolved in 90 ml water, attenuated to final pH and volume made up to 100 ml; 1% GSH solutions of pH 3.0 and 6.5 were prepared by dissolving 50 mg of reduced glutathione in 5 ml of buffer at required pH; 0.01 and 0.1% GSH solutions were made accordingly. Oxytocin solution was prepared by adding 0.5 mg to the desired GSH solutions. The detailed protocol can be followed in Huck et al. (2006). For degradation of oxytocin by interaction with glutathione, oxytocin solutions (1%) were prepared by directly adding

1 mg oxytocin to 100 µl of GSH solutions (pH 3.0), which was considered as the starting point for kinetics. The mixture was incubated via a thermomixer (Thermomixer comfort, Eppendorf, Germany) at 37°C and 500 rpm for 3 h. Aliquots of 10 µl were taken after 0 and 180 min and were utilized directly for qualitative analysis. The remaining sample solutions were stored in a deep freezer at −20°C.

Near-infrared spectroscopy (NIRS)

NIR Fourier-Transform spectrometer (FT-NIR; Büchi, Flawil, Switzerland) equipped with a tungsten–halogen lamp and a lead sulphide (PbS) detector was employed for measurements. Two different cuvette types made of Suprasil (104-QS, V = 1400 µl; 115-QS, V = 400 µl; optical thin layer 10 mm; Hellma, Jena, Germany) were used for transmission measurements. The NIR instrument was connected with a standard 2 m optic glass fibre (silica glass, Infrasil, Bes. Optics Inc., Warwick, UK; optical thin layer 0.5, 1.0, 1.5, 2.0, 2.5, 3.0 mm). A single beam polarisation interferometer was used to select wavelength in a range from 1,000 to 2,500 nm (4,000–10,000 cm^{-1}). The instrument offered a resolution of 12 cm^{-1}, an absolute wavelength accuracy of ±2 cm^{-1} and a relative reproducibility of 0.5 cm^{-1}. Chemometric software (NirCal 4.21; Büchi) was used for pre-processing treatments of raw data, as data analysis tool for determining parameters and for unknown sample predictions. Principal component analysis (PCA) and factor analysis method were applied for data compression. Two basic chemometric methods i.e., partial least squares regression (PLSR) and principal component regression (PCR) were applied for linear regression. Spectra were split into a calibration set (67%) and a validation set (33%). The optimum number of factors was obtained by predicted residual error sum square (PRESS) function and quality of calibration was described by Q value. The following parameters were calculated to evaluate the success of data pre-treatment:

1. BIAS, the average deviation between predicted values (y_n) and actual values (x_n) in the calibration-set; should be close to zero.

$$\text{BIAS} = \frac{1}{N}\sum (x_n - y_n)$$

2. PRESS, the sum of the square of deviation between predicted and reference values. The PRESS value of the validation set should be as small as possible and similar to that of the calibration set.

$$\text{PRESS} = \sum (x_n - y_n)^2$$

3. Standard error of estimation (SEE), the standard deviation of differences between reference values and NIRS-results in calibration set.

$$\text{SEE} = \sqrt{\frac{1}{N}\sum (x_n - y_n - \text{BIAS})^2}$$

4. Standard error of prediction (SEP), the counterpart for test-set samples.

$$\text{SEP} = \sqrt{\frac{1}{N}\sum (x_n - y_n - \text{BIAS})^2}$$

SEE and SEP should be as small as possible.

5. The correlation coefficient (R^2) should approach 1.

For *quantitative NIRS analysis*, the glutathione containing solution was applied to pre-coated thin-layer chromatography (TLC) sheets (Polygram Sil G, 20 × 20 cm, Machery-Nagel, Düren, Germany) with concentrations ranging from 1,000 to 10,000 ppm in steps of 1,000 ppm. Mobile phase was comprised of 0.1% trifluoroacetic acid (TFA) and acetonitrile (ACN) (analytical reagent grade) 92:8 (v/v). The sheets were kept/soaked in mobile phase for 2 h, and afterwards they were dried in a furnace at 95°C for 15 min. Ninhydrin spray reagent (0.2% in isopropanol) was used for locating the glutathione spots.

For *qualitative NIRS analysis* GSH (1%, pH 3.0), oxytocin (1% in water) and a mixture of GSH and oxytocin after incubation were selected. At a particular stage, 2 µl of the solution was added on pre-coated TLC sheets (8 × 4 cm). A mixture of acetonitrile (ACN) and trifluoroacetic acid (0.1% TFA) at a ratio of 92:8 (v/v) was used as mobile phase. The samples and conjugates were located on TLC plates by immersing them in an iodine chamber.

Liquid chromatography coupled to UV-detection (LC-UV)

The LC-equipment was composed of a low-pressure gradient pump (Model 616, Waters), a controller (Model 600S, Waters), a column heater (Model TC 1900, ICI, Welshpool, Australia), a helium degassing system, an autosampler (Model 717 plus, Waters) and a photo diode array detector (DAD, Model 996, Waters) with 10 mm pathlength flowcell. Data was recorded on a data system (Millenium^{32}, Version 3.05.01, Waters) after separating GSH and its conjugates over a Phenomenex Luna C-18 column (250 × 4 mm I.D., 5 µm, 100 Å, Torrance, CA, USA) with mobile phase consisting of A: 0.1% trifluoroacetic acid (TFA) in water; B: ACN; linear gradient: 9–61% B in 22 min. The flow rate was 1.0 ml/min at a temperature of 40°C. Detection was accomplished at 214 nm with 20 µl of injected volume.

Liquid chromatography coupled to electrospray ionization mass spectrometry (LC-ESI-MS/MS)

For LC-ESI-MS/MS determinations, a low-pressure gradient micropump (Model Rheos 2000, Flux, Karlskoga, Sweden), a degasser (Model DG-301, Phenomenex, Torrance, CA, USA), a microinjector (Model CC00030, Valco, Houston, TX, USA) with 5 µl internal loop connected to quadrupole ion trap mass spectrometer (Model LCQ, Finnigan, San Jose, CA, USA) were used. The inner diameter of the separation column was adjusted to 2 mm (Phenomenex Luna C-18, 250 × 2 mm i.d., 3 µm, 100 Å, Torrance, CA, USA) to ensure an efficient ionization process. The applied flow rate was 200 µl/min, temperature 40°C and the volume injected 5 µl. Mobile phase consisted of A: 0.1% TFA in water; B: ACN; linear gradient: from 9% B to 61% B in 22 min. The following parameters were applied in all experiments: positive ion mode; source voltage, 4.52 kV; source current, 19.33 µA; sheath gas flow rate, 59.57 (Finnigan units; nitrogen); capillary voltage, 35.64 V; temperature of the heated capillary, 200°C; tube lens offset, −6.88 V; first octapole offset, −5.569 V; second octapole offset, −6.68 V. Data were recorded by XCalibur-Software (Finnigan).

Capillary electrophoresis (CE)

The CE experiments were carried out on a HP^{3D}-CE-System (Agilent Technologies, Waldbronn, Germany), equipped with a diode-array detector. For data processing a HP^{3D}-CE Chemstation (Rev. A.06.03, Agilent Technologies, Waldbronn, Germany) software package was used. The samples were detected at a wavelength of 192 nm. All separations were carried out by applying −30 kV at 22°C. Samples were injected at 50 mbar for 4 s by pressure injection. Polyimide coated fused silica capillaries (50 µm i.d. and 360 µm o.d., Polymicro Technologies, Phoenix, AZ, USA), with a total length of 60 cm and an effective length of 51.5 cm, were conditioned in steps by flushing with 0.1 M NaOH (20 min), water (15 min) and CE background electrolyte (BGE, 20 min). Prior to each run the capillary was purged (50 mbar) with the separation BGE for 5 min.

The BGE was prepared by 50 mM of sodium dihydrogen phosphate dissolved in water. The pH (pH-meter, WTW Multilab 540, Weilheim, Germany) was adjusted to 3.0 by adding phosphoric acid and finally 0.001% HDB was added as a EOF modifier. For analysis, the stock solution (see Sect. "Preparation of standard solutions") was diluted with the BGE in order to obtain the desired concentration.

Matrix assisted laser desorption/ionisation time-of-flight mass spectrometry (MALDI-TOF/MS)

The oxytocin conjugates of reduced glutathione (GSH) were prepared as explained above and subsequently spotted onto a stainless steel target (Bruker Daltonics GmbH, Bremen, Germany), followed by adding 1 µl of saturated α-Cyano-4-hydroxycinnamic acid (HCCA) in 50% (v/v) acetonitrile, 0.1% trifluoroacetic acid. Mass spectrometric measurements were carried out by MALDI-TOF/MS (Ultraflex MALDI TOF/TOF, Bruker Daltonics) in reflector mode. Data processing was accomplished by Flex analysis 2.4 post analysis software and data acquisition by Flex control 2.4. (Bruker Daltonics).

Results

Prior to analysis by near infrared spectroscopy (NIRS), the interaction of oxytocin with glutathione in buffers at pH 3.0 and 6.5 was verified via analysis by LC-UV, LC-ESI-MS and CE-UV.

Liquid chromatography coupled to UV-detection (LC-UV)

Oxytocin can form four conjugates with glutathione after splitting of the disulphide bridge, as described in Fig. 1. Conjugates 1 and 2 correspond to the single addition of glutathione to oxycotin at amino acid residues 1 and 6, respectively. Conjugate 3 results from adding two parts of glutathione to to one part of oxytocin and conjugate 4 represents an oxytocin dimer. After optimisation of chromatographic conditions, conjugates 1–4 were separated by reversed-phase liquid chromatography (RPLC) at 40°C, achieving short analysis time of less than 8 min. Phenomenex Luna C18 column (250 × 4 mm i.d., 5 µm, 100 Å) was employed as stationary phase and a gradient of ACN in 0.1%TFA was optimised in 22 min. Figure 2 shows the RP chromatogram of 0.05% oxytocin mixed with 1% GSH after 0 min (Fig. 2a) and 180 min (Fig. 2b). Figure 2b demonstrates that peaks 1 and 2 corresponding to conjugates 3 and 1, respectively, are already detected at the beginning of the reaction, other than the oxytocin peak (peak 3). After 3 h of incubation, the concentration of oxytocin (peak 3) is decreased and a new peak (peak 4 representing conjugate 2) emerged.

For quantitative consideration, a calibration curve based on a concentration range from 0.01 to 0.5 mg/ml for oxytocin and glutathione in pH 3.0 (stomach) and 6.5 (intestine) was established upon five consecutive injections of different concentrations. Found regression equations

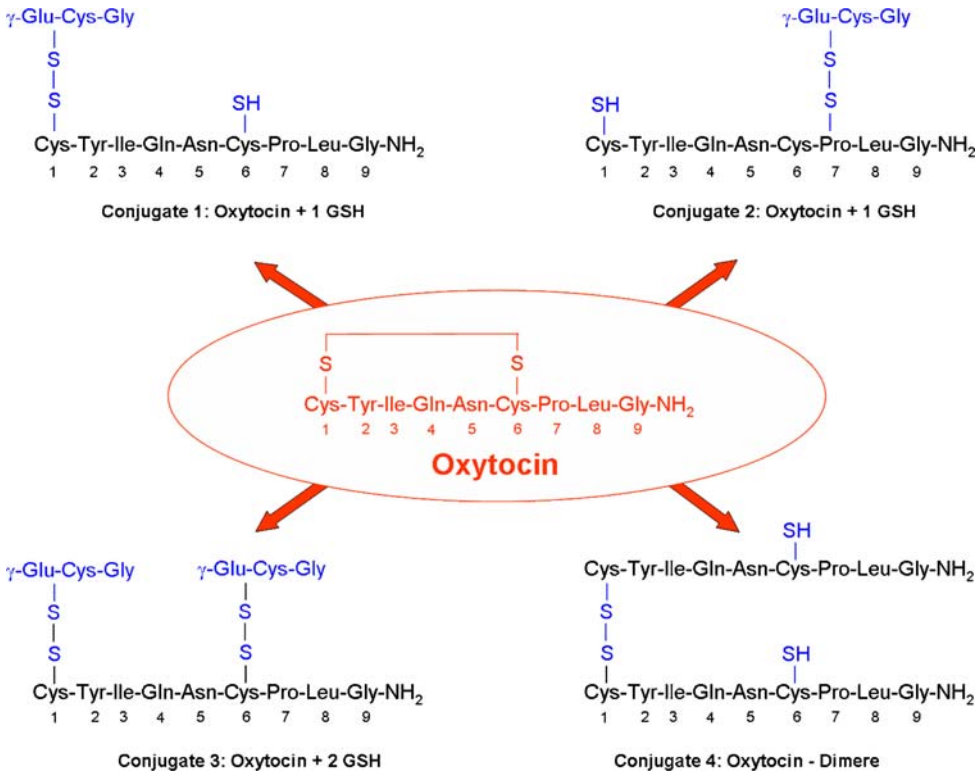

Fig. 1 Possible thiol-disulfide exchange reactions between oxytocin and glutathione

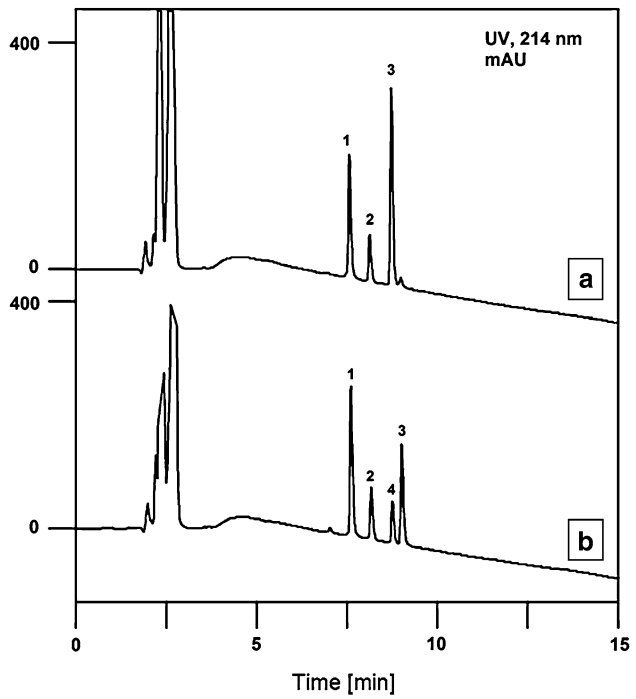

Fig. 2 RP-LC detection of 0.05% oxytocin incubated with 1% of glutathione at pH 3.0; at the beginning of the reaction (**a**) and after 180 min (**b**). Chromatographic conditions, as explained in experimental part; peak assignment, *1*: conjugate 3, *2*: conjugate 1, *3*: oxytocin, *4*: conjugate 2

were $y = 8E + 06x - 232929$ (pH 3.0) and $y = 8E + 06x - 119459$ (pH 6.5) with y being the area under the curve (AUC in mV × s) and x being the concentration in mg/ml (Table 1). The lower limit of detection (LOD) defined at a signal-to-noise ratio of 3 to 1 was found to be at 14.3 µg/ml for oxytocin; for glutathione it was at 5.8 µg/ml. The robustness of the separation system was confirmed by a relative standard deviation in percentage (%RSD) of the peak area being 1.79 intraday and 2.54% interday. Retention times showed 0.82 and 0.87% RSD intra- ($n = 5$) and interday (four subsequent days), respectively (Table 2). The kinetic degradation of 0.05% oxytocin at pH 3.0 with 0.01, 0.1 and 1% glutathione can be deduced from Fig. 3a. After 3 h of incubation, 0.01% glutathione showed an oxytocin degradation of 2%, in case of 0.1% glutathione a degradation of 19% and finally a degradation of 82% in case of 1% glutathione. Carrying out the same kinetic study at pH 6.5 resulted only in a degradation of 5% in case of incubation with 1% glutathione (Fig. 3b; Table 3).

Liquid chromatography electrospray ionisation mass spectrometry (LC-ESI-MS)

For a distinct peak assignment, the optimised LC system was coupled to mass spectrometry via an electrospray ionisation (ESI) interface. To allow for increased ionisation efficiency, the column inner diameter was reduced from 4

Table 1 Calibration results obtained for LC-UV, LC-ESI-MS, CE-UV, NIRS

Compound	pH	Concentration range (μg/ml)	Slope	Intercept	r^2	LOD (μg/ml)[a]	LOQ (μg/ml)[b]
LC-UV							
Oxytocin	3	10–50	8×10^6	−232929	0.9986	14.3	4.21
	6.5		8×10^6	−119459	0.9992		
LC-ESI-MS							
Glutathione	3	Okt.50	7×10^4	4×10^6	0.9898	1.93	3.93
	6.5		8×10^4	4×10^6	0.9899		
Oxytocin	3		5×10^4	6×10^6	0.9888	2.51	7.39
	6.5		6×10^4	5×10^6	0.9968		
CE-UV							
Glutathione	3	15–250	0.3732	−0.4007	0.9984	1.57	4.45
Oxytocin	3	15–250	11.012	−29.02	0.9906	11.05	32.85
NIRS							
Glutathione	3	1,000–10,000	0.986	76.64	0.9951	200	550

[a] The LOD defined at a signal to noise ratio of 3:1

[b] The LOQ defined at a signal to noise ratio of 9:1

Table 2 Validation results obtained for LC-UV, LC-ESI-MS, CE-UV

Time/pH	Compound	Intraday reproducibility (n = 5)		Interday reproducibility (n = 4 days)	
		Migration time RSD (%)	Peak area RSD (%)	Migration time RSD (%)	Peak area RSD (%)
	LC-UV				
T0	Oxytocin	0.82	1.79	0.87	2.54
	LC-ESI-MS				
T0	Glutathione	1.21	1.98	3.60	2.10
	Oxytocin	1.44	2.01	3.21	1.95
T3	Glutathione	1.31	1.99	2.71	4.29
	Oxytocin	1.52	2.16	2.86	3.95
	CE-UV				
T0	Glutathione	0.80	2.10	3.50	2.00
	Oxytocin	1.00	1.50	3.10	1.90
T3	Glutathione	0.50	0.40	2.50	4.50
	Oxytocin	0.70	1.20	2.90	3.90

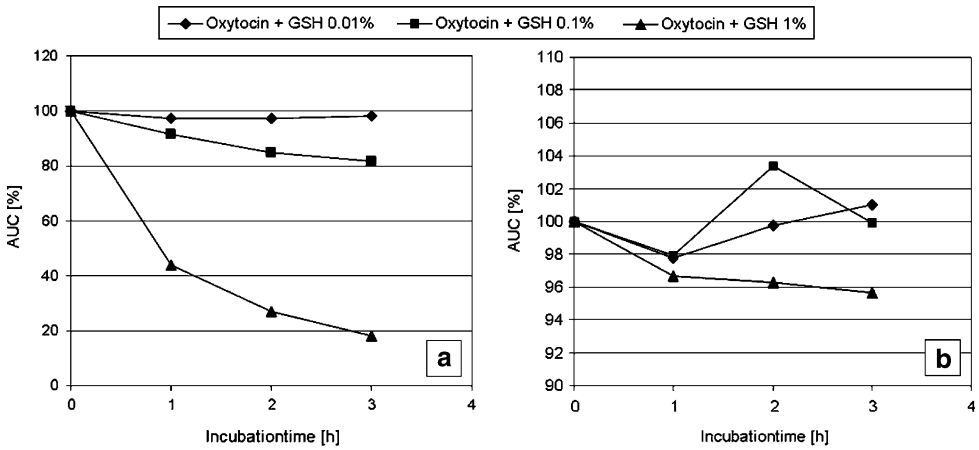

Fig. 3 Kinetic of oxytocin degradation by reaction with GSH in pH 3.0 buffer solution. Reaction of 0.05% oxytocin with different concentrations of GSH at **a** pH 3.0 and **b** pH 6.5

to 2 mm. Optimisation of mass spectrometric adjustments lead to the total ion stream chromatogram depicted in Fig. 4a upon injecting 0.05% oxytocine incubated with 1% glutathione at pH 3.0. Upon extraction of mass traces, the trace m/z = 1007.00–1008.00 corresponds to oxytocin (Fig. 4b), the ion trace of m/z = 1314.00–1315.00 refers to

Table 3 Degradation of oxytocin with glutathione over time def. by LC-UV, LC-ESI-MS, CE-UV, NIRS

Compound	pH	Degradation (%)
LC-UV		
Oxytocin	3	82
	6.5	5
LC-ESI-MS		
Oxytocin	3	78
	6.5	7
CE-UV		
Glutathione	3	44
Oxytocin	3	21
NIR		
Glutathione	3	28

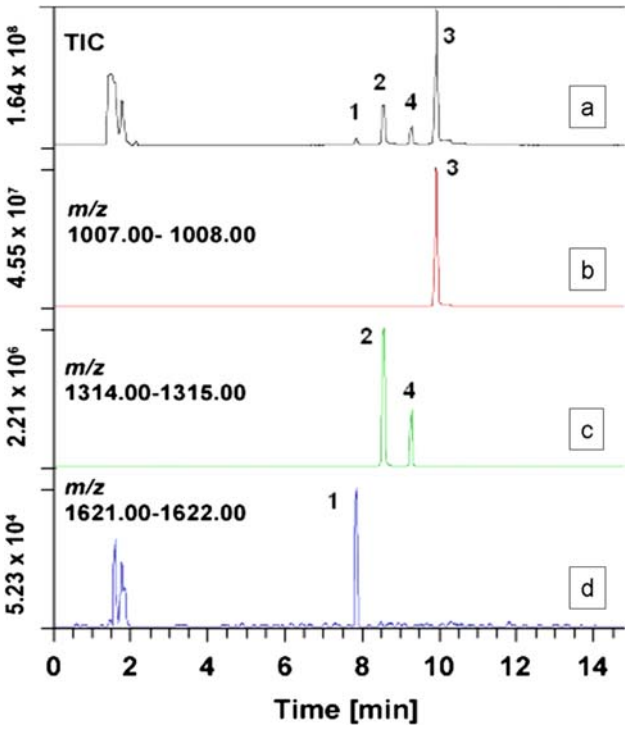

Fig. 4 RP-LC-ESI-MS after 180 min. incubation of 0.05% Oxytocin with 1% glutathione (pH 3.0); **a** TIC, **b** *m/z* = 1007.00–1008.00, oxytocin, **c** *m/z* = 1314.00–1315.00, conjugate 1 and 2, **d** *m/z* = 1621.00–1622.00, conjugate 3. Chromatographic conditions, according to the experimental part

conjugates 1 and 2 (Fig. 4c) and the trace *m/z* = 1621.00–1622.00 concerns conjugate 3 (Fig. 4d). Calibration equations for oxytocin and glutathione, respectively, were $y = 53649x + 6E + 06$ at pH 3.0 and $y = 63845x + 5E + 06$ at pH 6.5. The limit of detection of 2.5 µg/ml for oxytocin and 1.9 µg/ml glutathione (Table 1) was lower than that detected with LC-UV measurements, irrespective of pH. Interday and intraday reproducibility was

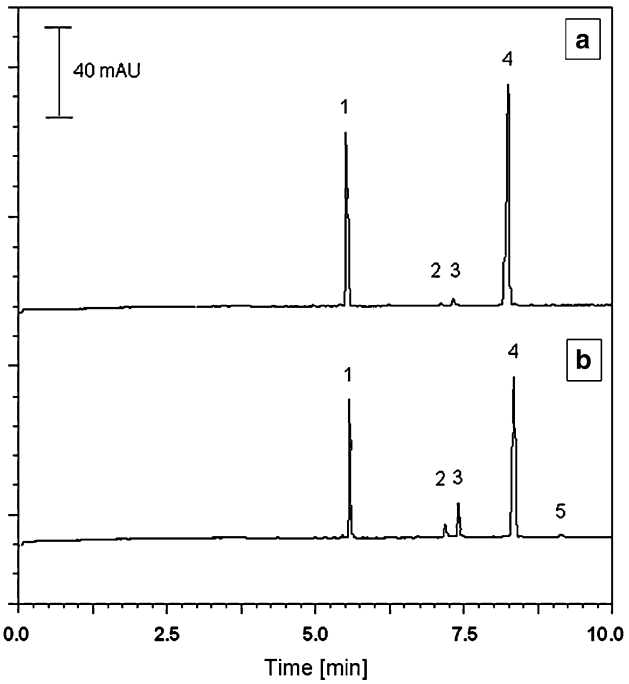

Fig. 5 Electropherogramm of 0.1% oxytocin incubated with 0.1% glutathione (pH 3.0) at **a** startpoint and **b** after 3 h of incubation. Conditions as described in the experimental part

determined as described above and found to be 4.3 and 1.52% maximal for peak areas and 3.60 and 2.16% for retention times, respectively (Table 2). Determination of oxytocin degradation over time resulted in a 78% degradation at pH 3.0 and 7% at pH 6.5 (Table 3), which corresponds to the results obtained by LC-UV.

Capillary electrophoresis coupled to UV-Detection (CE-UV)

Capillary electrophoresis offers the possibility to determine the degradation of oxytocin on the basis of a different separation principle compared to the described LC method. For the analysis of oxytocin, glutathione and conjugates 1–4, an optimised buffer system consisting of 50 mM sodium dihydrogen phosphate at pH 3.0 and 0.001% HDB as EOF modifier was applied.

In order to evaluate method precision, linearity, detection limits (LOD) and reproducibility were determined. For quantitative determination, calibration plots of peak area versus concentration of both analytes were obtained by linear regression. Analysis was carried out for at least five data points per concentration in a range from 15–250 µg/ml for glutathione and oxytocin. Slope, intercept, regression coefficient (r^2) and LOD can be deduced from Table 1. Calibration curves show excellent linear behaviour over the concentration range, with the LOD defined at an S/N of 3:1

of 1.57 μg/ml for glutathion and 11.05 μg/ml for oxytocin, respectively (Table 1). In order to investigate intraday and interday reproducibility after 4 consecutive days ($n = 4$ days) in respect of peak area and migration time, 10 μl of the standard mixture (glutathione (0.1%) and oxytocin (0.1%) diluted in 40 μl BGE was analysed five times ($n = 5$) as already described . The method was proven to be highly reproducible with RSD lower than 2.1% for intraday and 4.5% interday measurements. Measurements were based on migration time and peak area. Summarized results are highlighted in Table 2.

To analyse the interactivity of oxytocin with glutathione over time, electropherograms of the injected reaction mixtures obtained at the starting point and after 3 h of incubation at 37°C were recorded. In Fig. 5a, the starting point of the injected glutathione (peak 1) and oxytocin (peak 4) mixture is depicted. Due to the slow onset of the incubation process, only slight peaks can be detected (peaks 2 and 3 corresponding to conjugates 3, 1 and 2). After 3 h of incubation (see Fig. 5b), a reduction of peak 1 (glutathione) and peak 4 (oxytocin) can be noted. An increase of peak 2 (conjugate 3), peak 3 (conjugates 1 and 2) and peak 5 (conjugate 4) can be observed. After 3 h of incubation, 0.025% of glutathione showed a degradation of 44% and 0.025% of oxytocin indicated a degradation of 21% (Table 3).

Near infrared spectroscopy (NIRS)

Sample selection and optimisation of experimental parameters

1% reduced glutathione (GSH) in buffer at pH 3.0 and pH 6.5 and two buffer solutions at pH 3.0 (stomach) and pH 6.5 (cells) underwent optimisation. Neither samples containing different buffer solutions at different pH nor buffer solutions with and without glutathione led to differences in NIR spectra. This observation is due to the strong absorption of the employed buffer in the NIR-region. Hence further measurements were made after separating GSH and its conjugates on TLC plates following an optimised procedure.

Optimisation of experimental parameters such as optical thin layer (OTL), number of scans and temperature, is an important issue in NIRS to reach highest sensitivity and selectivity. Deployment of optimum scan number is important to reach high signal-to-noise ratio. It is crucial to chose the most suitable sample temperature and keep it constant in order to ensure a maximum of reproducibility. Three different measurement options were investigated in a comparative study: transmission cell, optical light fibre and sample desk probe. Transmission cells enable sample analysis with large pathlength having a positive effect on the quality of NIR spectra of liquids with low concentrations. Employment of optical light fibres allows to analyse both liquids and solids. In addition to diffuse reflection analysis, spectra in transflection mode can be recorded meaning that light passes the sample and is then reflected back to the detector on a non absorbing surface. Especially the easy change of optical thin layer makes the transflection probe a useful tool for analysing solutions and emulsions. In the present study, the sample desk was favoured compared to the light fibre to perform measurements in diffuse reflection mode. In order to reach higher reproducibility, constant positioning of the TLC sample spots had to be maintained during spectra recording; therefore a horizontal sample desk was used.

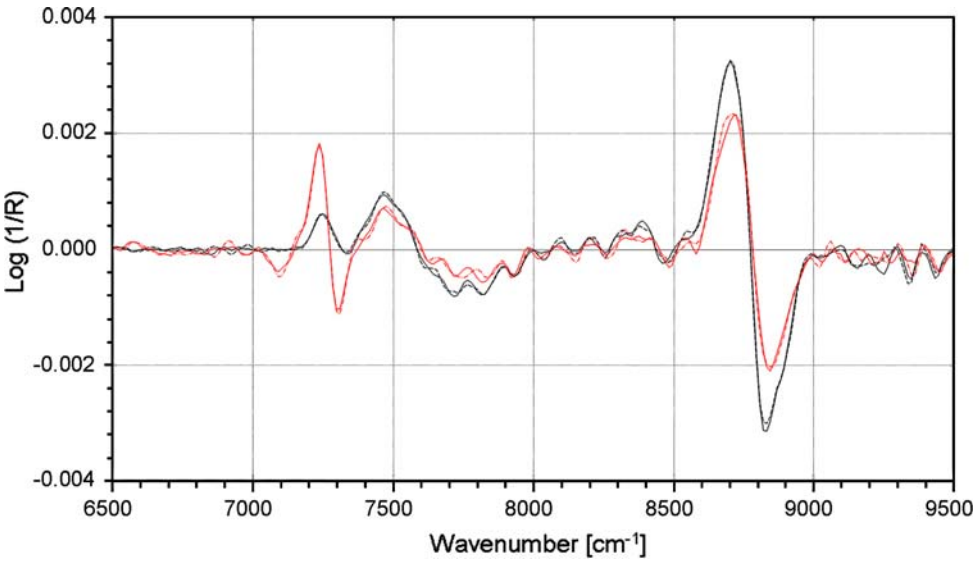

Fig. 6 Absorption spectra of buffer (*solid line*) and glutathione (pH 3.0) (*dashed line*); cuvette QS-104 ($V = 1{,}400$ μl)—black (*dark*) line, cuvette QS-115 ($V = 400$ μl)—grey (*light*) line; second derivative (Savitzky-Golay 9 points), 10 scans, $T = 23$°C

Measurement options and optical thin layer

Two transmission cell types (10 mm OTL, V = 1400 or 400 µl), the optical light fibre and the sample desk were modified and adjusted to find the best experimental setup for analysis.

Scans: Number of scans was varied from 10 to 320 and to 640 scans. As a result, spectra showed no notable shifts of wavenumber, but 3% deviation in peak intensities was noted changing from 10 to 150 scans. In the following experiments 10 scans were found to be sufficient.

Transmission cells: Comparison of spectra recorded with cell type QS-115 (V = 400 µl) indicated two additional peaks in contrast to spectra recorded with cell type 104-QS (V = 1400 µl). By pretreating the spectra, second derivative (Savitzky-Golay 9 Points), observable and interpretable differences such as shifts in wave number and baseline, could be observed. Band assignments showed a C–H and C=O stretching combination band at 4,548 cm^{-1} and a C–H stretching and bending combination band at 7,272 cm^{-1} (Fig. 6).

Optical light fibre: Solutions recorded in transflection mode were measured in a specially prepared glass stovepipe (V = 15 ml). Transflection bands showed high signal intensity in a low wavenumber range from 4,000 to 7,200 cm^{-1} at short path length (0.5 mm). In contrast, spectra recorded at large path length (3.0 mm) resulted in high signal intensities at higher wavenumber ranges (7,200 to 10,000 cm^{-1}). Figure 7a, c indicate five major peaks that can be attributed to applying different optical thin layers. Main excitations at around 4,188 cm^{-1} (Band 1) could be assigned to a second overtone of O–H stretching band. The combination bands of O–H bending and O–H stretching bands were located at 5,316 cm^{-1} (Band 2), 5,628 cm^{-1} (Band 3) and 7,164 cm^{-1} (Band 4), respectively. A band at 8,676 cm^{-1} (Band 5) could be assigned to a second overtone C–H stretching band (Fig. 7b).

Temperature: The influence of changing temperature on 1% GSH (pH 3.0) and buffer solutions (pH 3.0) was determined. Temperature was increased from 10 to 45°C in steps of 5°C each and adjusted with an accuracy of ±0.5°C. Figure 8 shows the difference between two main bands in terms of their deviating peak intensities. The band at 5,316 cm^{-1} could be assigned to a combination of a O–H stretching band whereas absorptions at 8,676 cm^{-1} point out the occurrence of a second overtone C–H stretching vibration. Numerous additional peaks were found at lower wavenumber around 4,344 cm^{-1} at short path length (0.5 mm). At higher wavenumber around 8,760 cm^{-1}, overlapping characteristic peaks were present due to larger path length (>1.5 mm). Because of inversion of spectra due to temperature changes at wavenumbers 5,290; 5,555; 6,950; 7,575 and 8,450 cm^{-1}, one optimal sample

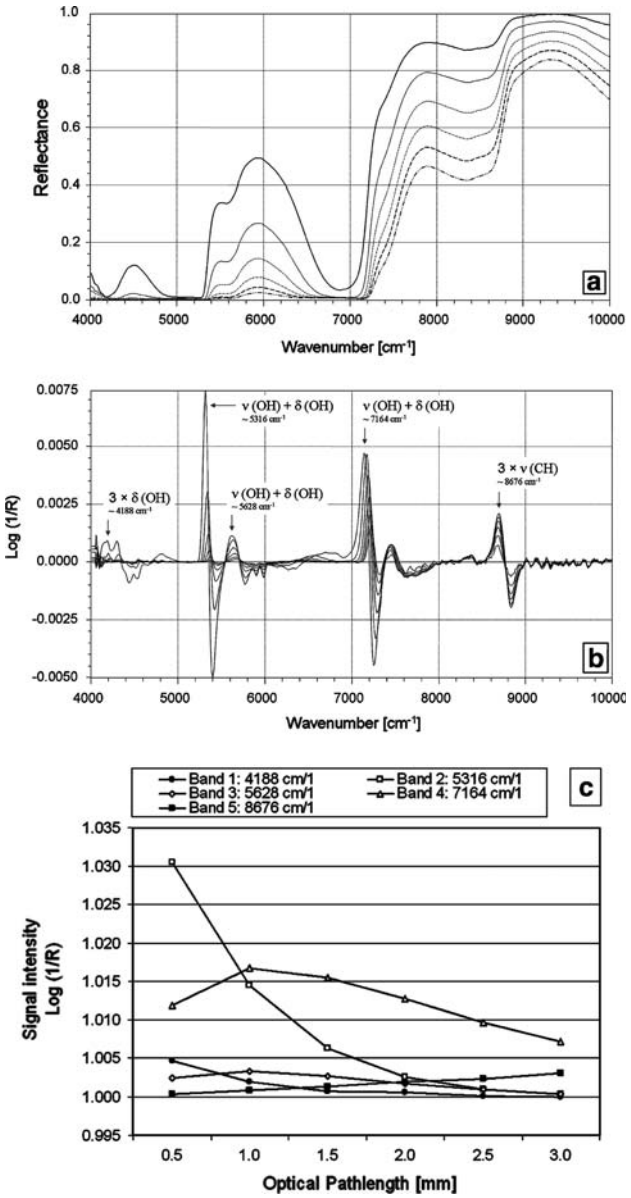

Fig. 7 Near-infrared reflection spectra of glutathione (pH 3.0) recorded with different optical thin-layers; fiber optic; optical thin-layers 0.5 (*solid line*), 1.0 (*thick dotted line*), 1.5 (*dashed line*), 2.0 (*dash dotted line*), 2.5 (*long dashed line*), 3.0 (*thin dotted line*) mm (**a**). Second derivative spectra of GSH in buffer (pH 3.0) marked with characteristic absorptions measured with optical thin layers from 0.5–3.0 mm, ν is for stretching- and δ for bending vibrations (**b**). Five major bands and its absorption characteristics at varying optical thin layers (**c**); 320 scans, T = 23°C

temperature could not be determined. However, absorption intensity increased at temperatures above 22°C, therefore sample measuring temperature was set to 23°C.

Generally, direct comparison of transmission, transflection and diffuse reflection measurements is not recommendable due to interfering absorption and reflection coefficients. Different scattering and absorption behaviour results in considerable shifts and irregularities in NIR

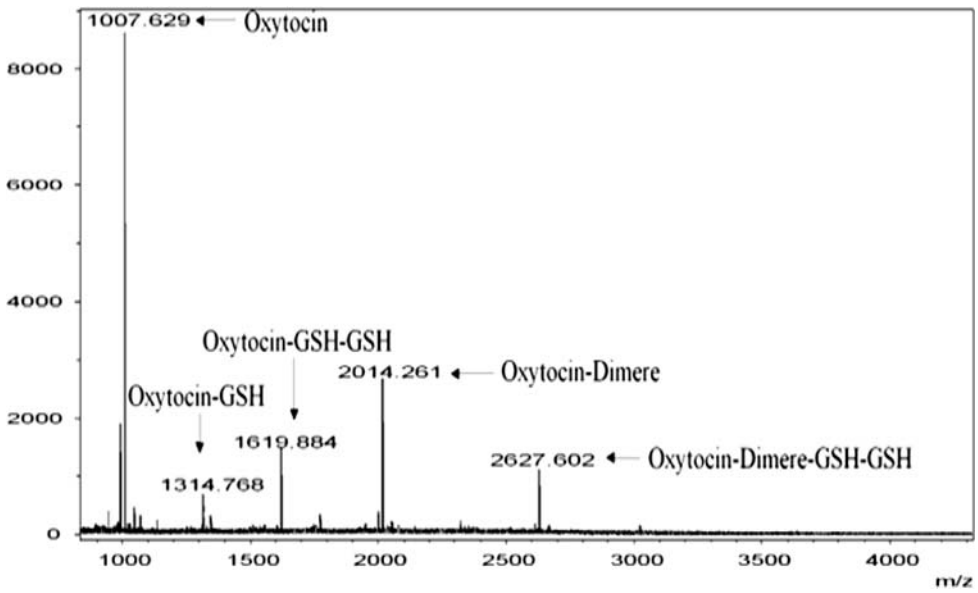

Fig. 8 MALDI/TOF-MS spectra of oxytocin and its conjugates recorded from *m/z* 900 to 4,000 by averaging 180 laser shots in reflector mode with HCCA as matrix

absorbance spectra and thus decreases reproducibility tremendously.

Qualitative analysis

GSH, oxytocin and the emerging conjugates (Fig. 1) were first separated by thin-layer chromatography (TLC) employing silica gel as a stationary and acetonitrile in 0.1% TFA at a ratio of 92:8 (v/v) as a mobile phase. Thereupon, near-infrared spectroscopic detection was employed for qualitative analysis. To be sure that all conjugates were separated and there was no overlapping of peaks, the corresponding spots were scraped from the TLC plate and after extraction into ACN analyzed via MALDI-TOF/MS as an additional experiment. Figure 8 shows the MALDI-TOF/MS spectra comprising the labeled masses of oxytocin and its conjugates. The spectra include the mass peaks for oxytocin that did not react/inert oxytocin (*m/z* 1007.629), oxytocin-GSH (*m/z* 1314.768), oxytocin-GSH–GSH (*m/z* 1619.884), the oxytocin dimer (*m/z* 2014.261) and oxytocin-dimer-GSH–GSH (*m/z* 2627.602). These peaks were then assigned to R_f values being 0.57 for oxytocin, 0.31 for oxytocin-GSH, 0.77 for oxytocin-GSH–GSH and 0.15 for the oxytocin-dimer. Subsequently, the identified spots were measured directly with the NIR sample desk probe in diffuse reflection mode. Calibration wavelength was selected in a range from 5,088 to 5,280 cm^{-1}. The model was calculated by PCA algorithm on the basis of three principal components. A *Q* value of 0.8958 attests to a highly accurate, robust and reliable model that can be used for further predictions and classifications of unknown samples. Figure 9a represents the two-dimensional score plot, whereas Fig. 9b gives an idea

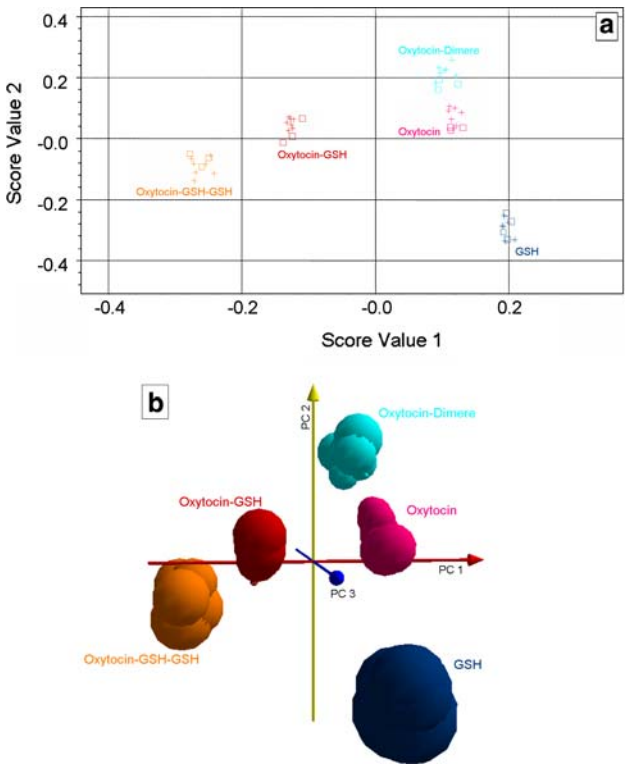

Fig. 9 Two-dimensional (**a**) and three-dimensional (**b**) score plot of oxytocin and its emerged conjugates spectra recorded directly from TLC-sheet, 10 scans, $T = 23°C$

about the separation of oxytocin and conjugates through a three-dimensional cluster model.

Quantitative analysis

A model for the quantitative analysis of conjugates 1–4 by employing TLC-NIRS was established. The calibration

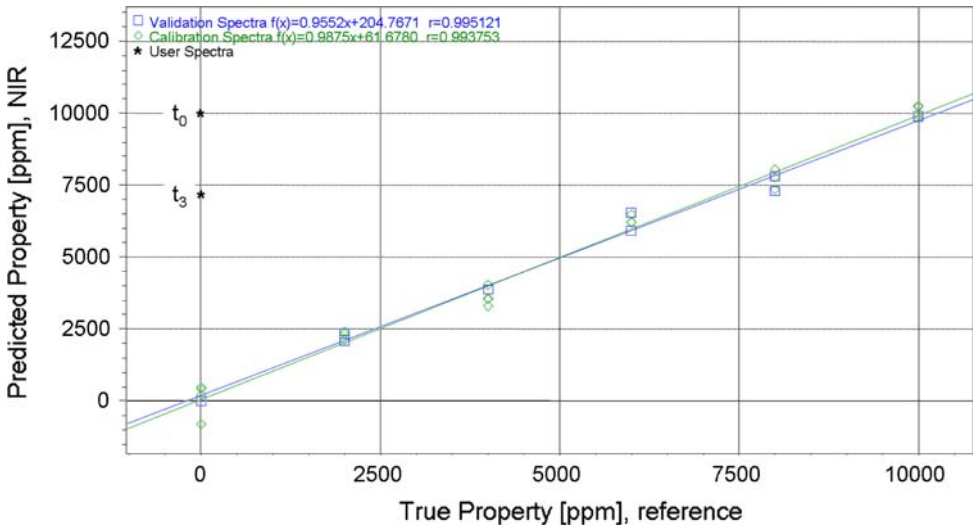

Fig. 10 Coherence between predicted property values (NIR) and true property values (reference) for the degradation of GSH calculated by principal component regression (PCR)—$R^2 > 0.99$. Spectra recorded directly from TLC-sheet, 10 scans, $T = 23°C$

data from varying amounts of glutathione was acquired by recording the spectrum of the TLC spots via NIR sample desk in diffuse reflection. Every spot was examined five times (10 scans). Calibration was calculated by principal component regression (PCR) algorithm on the basis of six principal components (C-set regression coefficient 0.9950, V-set regression coefficient 0.9930). The standard error of estimation (SEE) and the standard error of prediction (SEP) were quite analogous, which permitted robust calibration and good prediction. A consistency value of 115.445 confirmed high robustness of the calibration and a Q value of 0.781 demonstrated high linearity and good correlation between reference values and values calculated by PCR (Fig. 10). The detection limit of NIR Fourier-transform spectrometer was found to be at 200 µl/ml (200 ppm).

Discussion

The employment of NIRS as a TLC detector offers an efficient alternative to liquid chromatographic and capillary electrophoretic analysis for peptide reaction monitoring. The recorded fingerprint in the near infrared region allows for a selective distinct qualitative identification of conjugates without the need for expensive instrumentation such as quadrupole or MALDI-TOF mass spectrometers. The formation of novel conjugates can be monitored without the necessity to apply external pressure as in LC or an electric field like in CE, which might directly have an influence on the stability of the disulphide bondage. Thereby, it has to be kept in mind that the sensitivity of the NIRS method is lower than of the LC-UV, LC-ESI-MS and CE-UV methods. Limits of detection in NIRS of GSH were 200 µg/ml compared to 1.93% in LC-ESI-MS and 1.57% in CE-UV. Highest sensitivity was obtained in CE-UV. Regression coefficients showed comparable results applying LC-UV, LC-ESI-MS, CE-UV and NIRS.

Determination of the percentage of degraded oxytocin resulted in similar results for LC-UV and LC-ESI-MS, namely 82 and 78%, respectively. In CE-UV, 21% degradation was found, which might be explained by the applied electric field within the capillary. Through NIRS, the degradation percentage of glutathione was found to be 28%.

Acknowledgments The Austrian Nano-Initiative co-financed this work as part of the Nano-Health project (no. 0200), the sub-project NANO-N-0204 being financed by the Austrian FWF (Fonds zur Förderung der Wissenschaftlichen Forschung) (Project no. N-0204-NAN).

References

Alexander T, Tran DC (2001) Near-infrared spectrometric determination of di- and tripeptides synthesized by a combinatorial solid-phase method. Anal Chem 73:1062–1067

Amerov AK, Chen J, Small GW, Arnold MA (2005) Scattering and absorption effects in the determination of glucose in whole blood by near-infrared spectroscopy. Anal Chem 77:4587–4594

Axon TG, Brown R, Hammond SV, Maris SJ (1998) Focusing near infrared spectroscopy on the business objectives of modern pharmaceutical production. J Near Infrared Spectrosc 6:A13–A19

Barabás B (1998) A simple testing prodecure for near infrared instruments. J Near Infrared Spectrosc 6:A163–A170

Bokobza L (1998) Near infrared spectroscopy. J Near Infrared Spectrosc 6:3–17

Burns DA, Ciurczak EW (1992) Handbook of near-infrared analysis. Marcel Dekker, New York

Camera E, Picardo M (2002) Analytical methods to investigate glutathione and related compounds in biological and pathological processes. J Chromatogr B 781:181–206

Chen QU, Zhao J, Zhang H, Wang X (2006) Feasibility study on qualitative and quantitative analysis in tea by near infrared spectroscopy with multivariate calibration. Anal Chim Acta 572:77–84

Ciurczak EW, Drennen JK (2002) Pharmaceutical and medical applications of near-infrared spectroscopy. Marcel Dekker, New York

De la Haba MJ, Garrido-Varo A, Guerrero-Ginel JE, Pérez-Marín DC (2006) Near-infrared reflectance spectroscopy for predicting amino acids content in intact processed animal proteins. J Agric Food Chem 54:7703–7709

Delpy DT, Cope M (1997) Quantification in tissue near-infrared spectroscopy. Phil Trans R Soc Lond B 352:649–659

Esbensen KH (2001) Multivariate data analysis in practice, 5th edn. Aalborg University, Esbjerg

Fernández-Ahumada E, Garrido-Varo A, Guerrero-Ginel JE, Wubbels A, Van der Sluis C, Van der Meer JM (2006) Unterstanding factors affecting NIR-analysis of potato constituents. J Near Infrared Spectrosc 14:27–35

Forina M, Casolino MC, de la Pezuela Martinez C (1998) Multivariate calibration: applications to pharmaceutical analysis. J Pharm Biomed Anal 18:21–33

Guggenbichler W, Huck CW, Kobler A, Popp M, Bonn GK (2006) Near infrared spectroscopy, cluster and multivariate analysis—contributions to wine analysis. J Food Agri Environ 4(2):98–106

Heigl N, Huck CW, Rainer M, Ul-Haq N, Bonn GK (2006) Near infrared spectroscopy, cluster and multivariate analysis hyphenated to thin layer chromatography for the analysis of amino acids. Amino Acids 31:45–53

Herschel W (1800) Investigation of the powder of the prismatic colours to heat and illuminate objects. Phil Trans 255–283

Huck CW, Maurer R, Popp M, Basener N, Bonn GK (1999) Quantitative Fourier transform near infrared reflectance spectroscopy (NIRS) compared to high performance liquid chromatography (HPLC) of a flavone in Primulae veris Flos extracts. Pharm Pharmacol Lett 9(1):26–29

Huck CW, Guggenbichler W, Bonn GK (2005) Analysis of caffeine, theobromine and theophylline in coffee by near infrared spectroscopy (NIRS) compared to high-performance liquid chromatography (HPLC) coupled to mass spectrometry. Anal Chim Acta 538(1–2):195–203

Huck CW, Pezzei V, Schmitz T, Bonn GK, Bernkop-Schnürch A (2006) Oral peptide delivery: are there remarkable effects on drugs through sulfhydryl conjugation? J Drug Target 14(3):117–25

Lauridsen RK, Everland H, Nielsen FL, Engelsen SB, Norgaard L (2003) Exploratory multivariate spectroscopic study on human skin. J Chromatogr 9:137–146

McIntosh LM, Summers R, Jackson M, Mantsc HH, Mansfield JR, Howlett M, Crowson AN, Toole JWP (2001) Towards non-invasive screening of skin lesions by near-infrared spectroscopy. J Invest Dermatol 116:175–181

Miyazawa M, Sonoyama M (1998) Second derivative near infrared studies on the structural characterization of proteins. J Near Infrared Spectrosc 6:A253–A257

Morgenstern I, Kirch W (2003) Das glutathionsystem im menschlichen gastrointestinaltrakt. Dtsch Med Wochenschr 128:507–511

Pezzaniti JL, Jeng TW, McDowell L, Oosta GM (2001) Preliminary investigation of near-infrared spectroscopic measurements of urea, creatinine glucose, protein, and ketone in urine. Clin Biochem 34:239–246

Reich G (2003) Near infrared spectroscopy and imaging: basic principles and pharmaceutical applications. Adv Drug Del Rev 57:1109–1143

Schmitz T, Huck CW, Bernkop-Schnürch A (2006) Characterisation of the thiol-disulphide chemistry of desmopressin by LC, μ-LC, LC-ESI-MS and Maldi-Tof. Amino Acids 30(1):35–42

Siesler HW, Ozaki Y, Kawata S, Heise HM (2002) Near-infrared spectroscopy principles, instruments, applications. Wiley–VCH, Germany

Sissons M, Osborne B, Suissons S (2006) Application of near infrared reflectance spectroscopy to a durum wheat breeding programme. J Near Infrared Spectrosc 14:17–25

Shaw RA, Kotowich S, Mantsch HH, Leroux M (1996) Quantitation of protein, creatinine, and urea in urine by near-infrared spectroscopy. Clin Biochem 29(1):11–19

Shaw RA, Mansfield JR, Kupriyanov VV, Mantsch HH (2000) In vivo optical/near-infrared spectroscopy and imaging of metalloproteins. J Inorg Biochem 79:285–293

Sowa MG, Kohlenberg E, Payettw JR, Leonardi L, Levasseur MA, Riley CB (2006) Detecting intestinal ischemia using near infrared spectroscopy. J Near Infrared Spectrosc 14:1–7

Tran DC, Kong X (2000) Near-infrared spectrophotometric determiantion of tri- and tetrapetides. Anal Biochem 286:67–74